



A review on design and performance of thermomagnetic devices

Ravi Anant Kishore*, Shashank Priya

Center for Energy Harvesting Materials and Systems (CEHMS), Virginia Tech, Blacksburg, VA 24061, USA



ARTICLE INFO

Keywords:

Energy harvesting
Thermomagnetics
Thermoelectrics
Soft magnet
Magnetocaloric
Curie engine

ABSTRACT

Thermomagnetic energy harvesting technology has not received significant attention despite great potential for generating electricity from low thermal gradient near room temperature. This review summarizes the findings reported in literature covering the broad topical areas within thermomagnetic energy harvesting and provides perspective on the potential applications of this technology. The information has been organized chronologically in order to provide systematic understanding of the concepts and evolution of the device designs. Both, active and passive types of thermomagnetic energy harvesters have been included in the paper. The selection of suitable thermomagnetic material is key towards achieving an efficient energy generation device. Therefore, various material compositions have been discussed and their thermomagnetic behavior has been elucidated to provide guidance for their implementation in future devices.

1. Introduction

All forms of energy, such as mechanical, electrical, magnetic, or metabolic, ultimately degrade to thermal energy. Therefore, thermal energy is considered as one of the most ubiquitous forms of available energy. Unfortunately, in most cases, a significant fraction of available thermal energy is discarded as waste heat. Vehicles, manufacturing and power plants, electrical and electronic devices, or the human body emit thousands of joules of heat that is discarded in the environment. According to an estimate by the US Department of Energy (DOE), almost 50% of thermal energy generated from all fuels burned remains unused and is released into the atmosphere. Wasted thermal energy from US industries could generate up to 20% of the domestic electrical supply [1].

Utilizing the wasted thermal energy and converting it into more usable form, such as mechanical or electric energy, has been an interesting area of research for last few decades. Currently, the popular low-temperature thermal energy conversion mechanism is based upon thermoelectric (TE) effect. TE converters utilize Seebeck effect, where a voltage is induced when the hot ends of two dissimilar conductors are connected at a junction [2]. TE converters have relatively low energy-conversion efficiency, ~5% when hot-side temperature is below 200 °C, which limits their application especially where reliability is a major consideration [2,3]. The most common TE converters consist of bismuth telluride (Bi_2Te_3) that exhibits figure of merit (ZT) close to unity [4]. It has been proposed [5] that TE converters should have at least 3 times higher efficiency than the current state-of-the-art to become cost-effective.

A fundamentally different approach for converting thermal energy into other usable form of energy is thermomagnetic energy generation (TMEG). TMEG is based on the effect of heat on magnetic properties of ferromagnetic materials which undergo sharp phase change near the transition temperature. The transition temperature, also termed as Curie temperature or Curie point, of ferromagnetic materials refers to the condition where magnetization disappears and material transforms into paramagnetic state. Rapid change in magnetization around a specific temperature can be used to design a device that converts thermal energy into electrical energy, either directly or indirectly via mechanical energy.

The effect of heat on magnetic properties of ferromagnetic material has been known for a long time. Few Patents issued in late 19th century describe concepts for converting heat into mechanical or electrical energy [6–9]. Unfortunately, the performance of these thermomagnetic devices was low and consequently, they were not used for any domestic or industrial application. In addition, limited studies in 1950s [10–12] demonstrated that the theoretical limit for thermal-to-electrical energy conversion efficiency of thermomagnetic devices was less than 1%. These studies reduced interest in this area for several decades [13]. In past couple of decades, there were some attempts made to revive this technology primarily owing to advances made in design of high performance magnetic materials and understanding of thermal transport interfaces.

With advancements in low-power electronics, the energy requirements for commonly utilized devices have reduced. The wireless sensors, for example, now require less than 1 mW to operate. For

* Correspondence to: Virginia Tech., 310 Durham Hall, Blacksburg, VA 24061, USA.
E-mail address: ravi86@vt.edu (R.A. Kishore).

several applications like remote location and hard-to-reach areas, it is quite difficult to power the electronic devices using grid electricity. In such applications, lithium ion batteries are currently used, which limits the durability of electronic devices and presents maintenance challenges. While the need for electrical energy is growing exponentially over time, growth in battery capacity is proceeding along a flattening S-curve [14]. Unarguably, there exists an urgent need for harvesting energy from natural resources. Thermomagnetic devices employing rare-earth magnetic materials can be designed to generate electricity near room temperature under very low thermal gradients. In addition, thermomagnetic devices can also be used as thermal actuators. A recent study by Chun et al. demonstrates that thermomagnetic devices can be used to enhance the cooling rate of solar modules utilized in solar-powered unmanned aerial vehicles (UAVs) [15]. Further, this study showed that thermomagnetic devices can be used to increase the heat dissipation rate of data storage servers [15]. Scaling of thermomagnetic generators to generate higher power can be targeted once the basic understanding of high efficiency design has been established.

The primary aim of this paper is to review the results reported in literature on thermomagnetic energy harvesting and to re-evaluate the potential of this technology. An attempt has been made to organize the information chronologically in order to provide comprehensive summary of fundamental concepts, modeling strategies, and device designs. There are usually two methodologies for converting thermal energy into electrical energy. The first method relies on direct energy conversion by using active thermomagnetic devices. The second method is based upon indirect energy conversion via mechanical energy by using passive thermomagnetic devices. Both these types of devices have been discussed in this paper in two separate sections. The selection of appropriate ferromagnetic material with respect to operating condition is key towards achieving good thermomagnetic energy conversion efficiency. The performance of conventional and non-conventional thermomagnetic materials has been compared and their usability is discussed in the context of current requirements.

2. Early thermomagnetic devices

In 1889, Nikola Tesla patented numerous designs for thermomagnetic motor under US Patent 396121 [6], as shown in Fig. 1(a). He obtained the mechanical energy by a reciprocating or rotary action resulting from combined effects of heat, magnetism, and a spring. Tesla's thermomagnetic motor had an electromagnet or a permanent magnet that generated magnetic field, which interacted with an armature. The armature was attached to an arm, which was free to rotate about a hinge. When armature was heated by a burner and its temperature increased above its Curie temperature, spring pulled the armature away from the permanent/electro-magnet. Eventually, the armature cooled below the Curie temperature and the magnetic force overcame the spring force bringing the armature back to its original position. This process continued as long as heating and cooling cycle continued.

Thomas Edison, in his US Patent 380100 [7], presented the concept as pyromagnetic motor (Fig. 1(b)), where the heat was generated from combustion of coal or wood. He employed thin iron sheet to construct an interstitial armature with interstices or tubes extending longitudinally through it. The armature was mounted vertically using a shaft and was placed between the magnetic poles of permanent or electro-magnets. A furnace was located beneath the armature, which had two outlets that covered the lower ends of some of the armature tubes on the opposite sides. Hot air from the furnace outlets was blown through these two group of tubes and cold air through the remaining group of tubes between the hot tubes. Hot tubes were on the diametrically opposite sides and cold tubes in the middle. The arrangement was such that it did not restrict the rotation of armature. Because of the temperature difference, the magnetization of armature varied among different sections, causing an unbalanced force. This led to continuous

rotation of armature as long as armature tubes were periodically heated and cooled.

In 1890, Nikola Tesla introduced a patent for pyromagnetic electric generator [8]. Unlike previous patents, his aim was to produce electric current directly without mechanical motion. As shown in Fig. 1(c), a permanent magnet was bridged by an armature core composed of some iron tubes. Two conductors, in which the electric current would develop, were coiled around the armature core. The central portion of armature core can be heated by a furnace beneath it and cooling can be achieved by the steam coming from a boiler. Alternate cooling and heating of the armature switched on and off the magnetic circuit causing variation in the magnetic field, which ultimately resulted in electrical current in the conductors.

In 1892, Thomas Edison patented another type of pyromagnetic generator [9] that contained bundles of thin iron tubes arranged circumferentially inside two iron rings, as shown in Fig. 1(d). Strong permanent magnet or electromagnets were used to magnetize these iron tube arrangements such that the rings formed the two poles of a long magnet. Each bundle of tubes was surrounded by a winding. A furnace was placed beneath the lower iron ring and a half disk-shaped shield was used to cover lower ends of some of the tubes. The open tubes received the hot air from the furnace and thus heated up. On the other hand, the tubes that were covered by the shield were protected from the heat of the furnace, and therefore they cooled down. The shield was slowly rotated about its axis using a motor so that the tubes were always thermally unstable. Progressive cooling and heating of the iron tubes caused change in their magnetization, which generated current in the windings.

It can be noticed from Fig. 1 that early thermomagnetic devices had very complex designs. In addition, they used iron as the working ferromagnetic material. Iron needs a very high temperature, around 700 °C, for demagnetization. Such high temperature will cause thermal degradation of the permanent magnet. Also, achieving such high temperatures requires combustion of lot of fuel, which questions the economic feasibility of these devices. Last but not least, the thermodynamic efficiency of heat engine is proportional to $\frac{\Delta T}{T}$, where T denotes the working temperature. Ferromagnetic to paramagnetic transition normally occurs in a narrow temperature range, therefore ΔT is small. However, as transition temperature increases the efficiency of thermomagnetic device decreases, which makes iron an unsuitable working material for thermomagnetic devices. Clearly, lack of suitable magnetic materials and complex designs resulted in slow progress of thermomagnetic devices.

3. Active thermomagnetic devices

Historically, the conversion of thermal energy into electrical energy is accomplished in two different ways. The first method is direct energy conversion and these type of systems are called as active thermomagnetic devices. They have been traditionally also called as thermomagnetic generator. The second conversion method is via intermediate mechanical stage and such systems are called as passive thermomagnetic devices. These will be discussed in the next section.

3.1. Working principle

A schematic diagram of thermomagnetic generator is shown in Fig. 2. In its simplest form, a thermomagnetic generator consists of a C-shaped permanent magnet or an electro-magnet, a ferromagnetic material placed as a shunt between the poles of permanent magnet, and a winding around the shunt material. The shunt is alternately heated and cooled through the Curie temperature (T_C) using a heat source and a heat sink. Increase in shunt temperature reduces the magnetization and therefore magnetic flux through the shunt decreases. Decrease in temperature produces the reverse effect. The

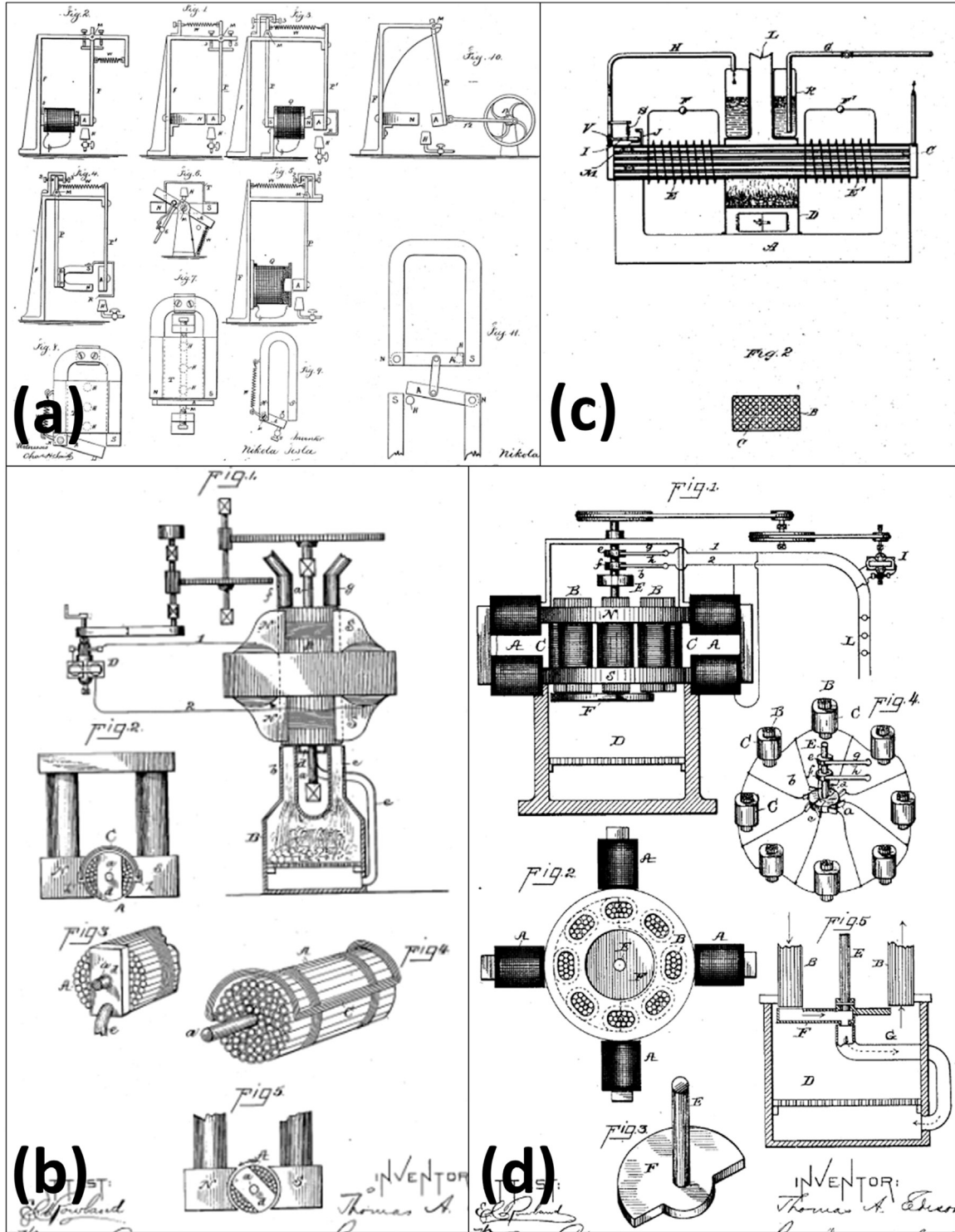


Fig. 1. Few early thermomagnetic devices. (a) Thermomagnetic motor by Nikola Tesla (US Patent 396121). (b) Pyromagnetic motor by Thomas Edison (US Patent 380100). (c) Pyromagnetic electric generator by Nikola Tesla (US Patent 428057). (d) Pyromagnetic generator by Thomas Edison (US Patent 476983).

continuously changing magnetic flux induces a voltage across the two ends of winding and electrical power is produced by cycling the shunt temperature.

If w_h and w_c are the electrical energy produced and q_{in} and q_{out} are heat-in and heat-out during the heating and cooling portions of thermal cycle, the efficiency of thermomagnetic generator can be defined as:

$$\eta = \frac{w_h + w_c}{q_{in}} \quad (1)$$

A study presented by Stauss [12] suggests that the maximum efficiency of a thermomagnetic generator can be estimated by assuming an infinitely long shunt material. A longer shunt requires lesser energy per unit volume to get magnetized at a given magnetic flux. Infinitely long shunt, therefore,

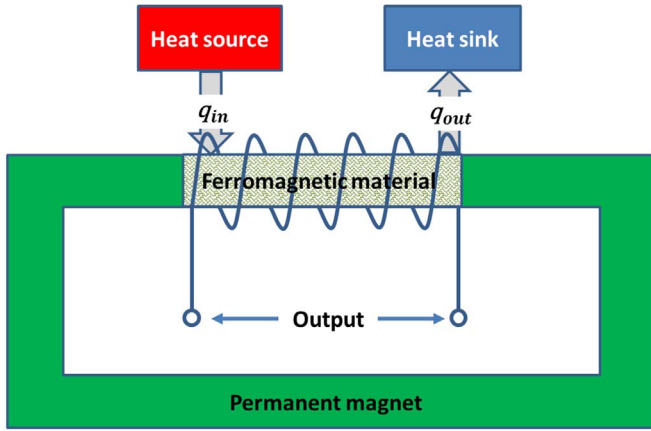


Fig. 2. Schematic diagram of a thermomagnetic generator.

puts an upper bound on the performance of device. Using Weiss theory of ferromagnetism, Stauss found that the maximum efficiency of a thermomagnetic generator can be expressed as [12]:

$$\eta_{max} \leq \frac{\pi H}{NI} \quad (2)$$

where H is average magnetic field due to permanent or electro-magnet, N is molecular field constant, I is intensity of magnetization, and NI is molecular field of ferromagnetic material.

Elliott [10] has proposed that maximum power output of a thermomagnetic generator can be expressed in terms of magnetic characteristics of the permanent magnet as:

$$P_{max} = \frac{1}{8} \omega V \mu_r H^2 \quad (3)$$

where it is assumed that the temperature of shunt varies in a sinusoidal manner at an angular frequency ω . Here V and μ_r denote volume and permeability of permanent magnet. This study also suggested that the efficiency of a thermomagnetic generator operating between shunt's upper temperature close to its Curie temperature ($T_h \approx T_C$) and shunt's lower temperature $T_c = T_C - \Delta T$ can be expressed as:

$$\eta = \frac{\pi}{4\sqrt{2}} \frac{\Delta T}{T_C} = 0.55 \times \text{Carnot efficiency}, \quad (4)$$

and the lowest shunt temperature $T_{c,min}$ can be given as:

$$T_{c,min} = \left[1 - \frac{B^2}{(4\pi)^2 \times 3 \times I_0^2} \right] T_C \quad (5)$$

where I_0 denotes intensity of magnetization of shunt material at 0 K and B is magnetic flux. Table 1 shows the thermomagnetic parameters of conventional ferromagnetic materials: cobalt, iron, and nickel along with efficiency of corresponding thermomagnetic generator model proposed by Elliott and Stauss per Eqs. (4) and (2) respectively. There are at least two important points that can be noted from the data shown in Table 1. First, the efficiency predicted by Stauss, per Eq. (2), is much lower than that predicted by Elliott per Eq. (4). Secondly, the thermomagnetic generator with common ferromagnetic materials has efficiency less than few percent.

Table 1

Performance of thermomagnetic generators using conventional ferromagnetic materials (thermomagnetic parameters taken from [16]) and Alnico I as permanent magnet ($H = 440$ Oe, $\mu_r = 6.5$, and $B \approx \mu_r H = 2860$ gauss; data taken from [12]).

	T_C (K)	I_0 (J = 1/2)	NI_0	ΔT (K)	η_{Carnot}	$\eta_{Elliott}$	η_{Stauss}
Fe	1043	1731	15.5×10^6	6.0	0.58%	0.32%	0.009%
Co	1393	1437	20.7×10^6	11.6	0.84%	0.46%	0.007%
Ni	631	508	9.4×10^6	42.2	6.69%	3.68%	0.015%

3.2. Alternatives for shunt material

Discovery of gadolinium turns out to be a new milestone in the development of thermomagnetic devices. Gadolinium is a rare-earth material exhibiting Curie temperature of ~ 293.2 K [17]. This permits gadolinium as working material in design of thermomagnetic generator for near room temperature operation. Using Eqs. (4) and (5), it can be calculated that thermomagnetic generator employing gadolinium as shunt and Alnico I as permanent magnet could theoretically operate in a very narrow temperature range 1.5 K and would have an efficiency of $\sim 0.29\%$. Though gadolinium based thermomagnetic generator has very low efficiency, the device could be used very effectively where heat supply is not constrained.

Multiferroic Heusler alloy, $\text{Ni}_{45}\text{Co}_5\text{Mn}_{40}\text{Sn}_{10}$, has been recently suggested as an alternative shunt material for thermomagnetic generators. The Heusler alloy has been found to have better efficiency than that of polycrystalline gadolinium, but it has high Curie temperature (408 K) [32] which limits the near-room temperature operation. Compositional modifications can be made to reduce the transition temperature; however, dopants will also have influence on the magnetic properties. More details on thermomagnetic materials is presented in Section 5.

3.3. Considerations for permanent magnet

Eq. (2) relates the maximum power output of a thermomagnetic generator with the magnetic characteristics of permanent magnet. Term $(\mu_r H^2)$ is used as a figure of merit for the selection of permanent magnet for thermomagnetic generator. Table 2 shows the figure of merit in the increasing order for some of the permanent magnets. The efficiency of thermomagnetic generator, however, is proportional to square of magnetic flux B . Fig. 3 depicts the efficiency of thermomagnetic generators employing gadolinium as shunt material at different magnetic flux density. All calculations were done assuming Curie temperature of gadolinium as 290 K and its intensity of magnetization at 0 K as $I_0 = 1800$ gauss. It can be seen that efficiency increases with increase in the value of B . It is evident that, in order, to achieve an efficient thermomagnetic generator, it is necessary to use a strong permanent magnet.

3.4. Thermomagnetic generator with regenerative heat exchanger

The studies on thermomagnetic generators so far were based on non-regenerative thermal cycle, which means that heat source and heat sink worked independently. Since the efficiency of thermomagnetic

Table 2

Figure of merit for various common permanent magnetic materials for use in thermomagnetic generators [10] (All units in CGS).

	H	μ_r	$\mu_r H^2$	$B \approx \mu_r H$
Chrom 3%	60	7	25,200	420
17% Cobalt	150	15.5	348,750	2325
Tungsten 6%	65	84	354,900	5460
Cunife I	500	1.5	375,000	750
36% Cobalt	240	12.2	702,720	2928
Indalloy sintered	240	12.5	720,000	3000
Cunife II	260	13	878,800	3380
Vectolite	900	1.2	972,000	1080
Alnico V	580	3	1,009,200	1740
Alnico I	440	6.5	1,258,400	2860
Cunico	660	3	1,306,800	1980
Alnico III	470	6.25	1,380,625	2938
Alnico II	560	6.2	1,944,320	3472
Alnico IV	700	4	1,960,000	2800
Alnico VI	750	4.5	2,531,250	3375
Alnico XII	950	4.5	4,061,250	4275

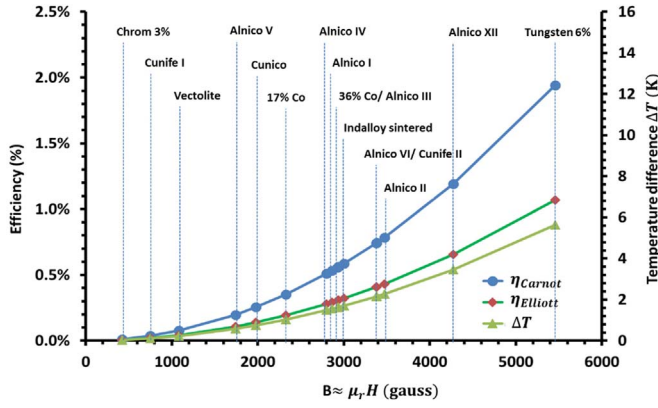


Fig. 3. Effect of magnetic flux density on performance of gadolinium based thermomagnetic generator. Different permanent magnetic materials have been indicated at appropriate magnetic flux density (data taken from [10]).

generators is quite low, this implies that a very small fraction of energy from heat source is converted into work while the majority is rejected to heat sink. An efficient thermomagnetic generator should have a regenerator to temporarily store the sensible heat released during the cooling portion of cycle and use it during heating.

Schematic diagram of regenerative thermomagnetic generator is shown in Fig. 4. It is similar to the normal thermomagnetic generator, except that it contains a regenerator. The function of regenerator is to preheat the heat source fluid by utilizing the returning heat sink fluid and thereby transferring part of q_{out} to heat source. In such case, net heat supplied q_h by the heat source and net heat rejected q_c to the heat sink can be given as:

$$q_h = q_{in} - q_r \quad (6)$$

$$q_c = q_{in} - q_r \quad (7)$$

where q_r is the regenerative heat.

The efficiency η_r of thermomagnetic generator with regenerator can be given as:

$$\eta_r = \frac{w_h + w_c}{q_h} = \frac{w_h + w_c}{q_{in} - q_r} \quad (8)$$

It can be shown mathematically that if regenerative heat is x times the sum of net heat-in and net heat-out, i.e. $q_r = x(q_{in} + q_{out})$, then

$$\eta_r = \frac{(1 + 2x)\eta}{1 + \eta x} \quad (9)$$

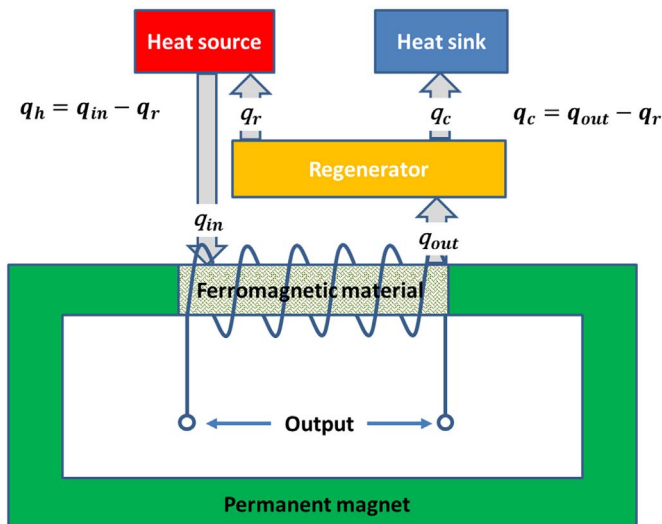


Fig. 4. A conceptual model of thermomagnetic generator with regenerator.

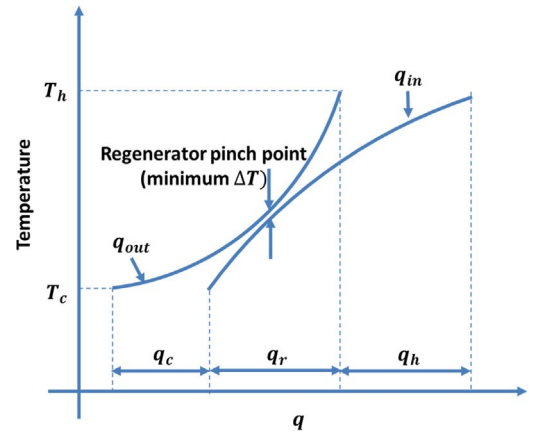


Fig. 5. Calculation of regenerated heat using T - q plane. The figure is reconstructed from reference [13] for illustration.

where $x = \frac{q_r}{q_h + q_c}$ and η is efficiency of a thermomagnetic generator without regeneration.

Kirol et al. [13] suggest that maximum possible regenerative heat for a regenerative thermomagnetic generator can be calculated using temperature-entropy diagram (T - S) of shunt during thermal cycle. The heat-in (q_{in}) and heat-out (q_{out}) are first determined by integrating TdS over heating and cooling portions of cycle respectively. The resulting heat curves are then positioned in a T - q plane in such a manner that at all temperatures, $q_{in} \geq q_{out}$, as shown in Fig. 5. All the points, where q_{out} is above q_{in} , energy to heat the shunt can be provided from rejected heat during cooling process of the previous cycle. Some additional heat (q_h) that must be provided by the heat source to heat the shunt up to temperature T_h is represented as portion of q_{in} which is not below q_{out} . Similarly, the net rejected heat q_c is represented as part of the curve q_{out} that is not above q_{in} . Depending on the regenerator's pinch point value, a vertical separation between q_{in} and q_{out} needs to be added.

Study by Kirol et al. [13] show that a zero-pinch point regenerative thermomagnetic generator with gadolinium shunt operating between $T_h = 290K$ (Curie temperature) and $T_c = 240K$ has efficiency of 8%, which is 47% of Carnot efficiency, at field strength of 400 kA/m (5026 Oe). The efficiency of generator increases to 12.8%, or 75% of Carnot efficiency, at field strength of 5.6 MA/m (70372 Oe). It should be noted that (as given by Eq. (4)) 55% of Carnot efficiency is theoretical limit for efficiency of a non-regenerative thermomagnetic generator. However, a regenerative thermomagnetic generator is capable of surpassing this theoretical limit and its performance approaches that of Carnot efficiency as the magnetic field is increased.

3.5. Performance improvement by cycling the magnetic field

In a traditional thermomagnetic generator, the working element, i.e. shunt material, experiences a fixed external magnetic field from the permanent or electro-magnet throughout the thermal cycle. Solomon [18] suggests that the efficiency of a thermomagnetic generator can be improved if the applied magnetic field is also cycled as the material is thermally cycled.

Fig. 6 shows the conceptual model of Solomon's thermomagnetic generator. The working ferromagnetic material is located inside the magnetic field region of a superconducting coil/solenoid. The material is energized and de-energized by a voltage source, and at the same time, it is heated and cooled in a cyclic manner such that there is a net gain of energy by the voltage source. The voltage v and the current i of the windings around the solenoid are related to magnetic fields B and H by:

$$v = nA \frac{dB}{dt} \quad (10)$$

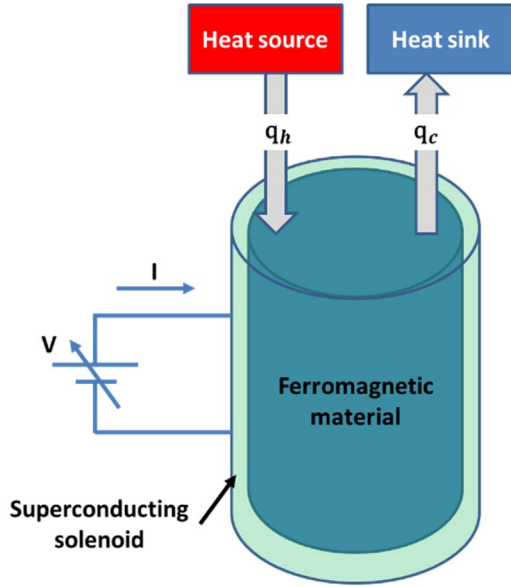


Fig. 6. A conceptual model of Solomon's thermomagnetic generator. The figure is reconstructed from reference [18] for illustration.

$$i = \frac{HL}{n} \quad (11)$$

where n is number of windings of solenoid, A is its cross-sectional area, $\frac{dB}{dt}$ is rate of change of magnetic induction in ferromagnetic material, R is resistance of wire, and L is length of solenoid. The magnetic induction B in ferromagnetic material is given as:

$$B(H, T) = \mu_0[H + M(H, T)] \quad (12)$$

where μ_0 is permeability of free space, H is applied magnetic field, and M is magnetization, which is function of applied field and its temperature. The power P and energy E supplied by voltage source to the unit volume of ferromagnetic element can be calculated as:

$$P = \frac{vi}{AL} = H \frac{dB}{dt} \quad (13)$$

$$E = \int P dt = \int H dB \quad (14)$$

Using Eq. (12), Eq. (14) can be modified as:

$$E = \mu_0 \int H dH + \mu_0 \int H dM \quad (15)$$

For a cyclic process, $\oint H dH = 0$. Therefore, the total energy E supplied by the voltage source during magnetic cycle is:

$$E = \mu_0 \oint H dM \quad (16)$$

If there is net gain of energy by the voltage source, then E calculated from Eq. (16) would be negative.

$$E_{out} = -\mu_0 \oint H dM \quad (17)$$

The working cycle of this thermomagnetic generator is demonstrated in Fig. 7, which is taken from reference [18]. It depicts the variation of magnetic field H against the magnetization M and M_s , where M_s denotes the magnetization of individual magnetic domains. When the applied magnetic field is smaller than the saturation field, i.e. $H < H_{sat}$, all the magnetic domains are not aligned and therefore, $M_s > M$. When the magnetic field reaches near or above the saturation field, M_s and M are equal.

Assuming that the applied field H during most of the cycle is large compared to saturation field H_{sat} , the area bounded by loop 1–2–3–4 is approximately equal to area 1'–2–3–4' and to simplify the calculation,

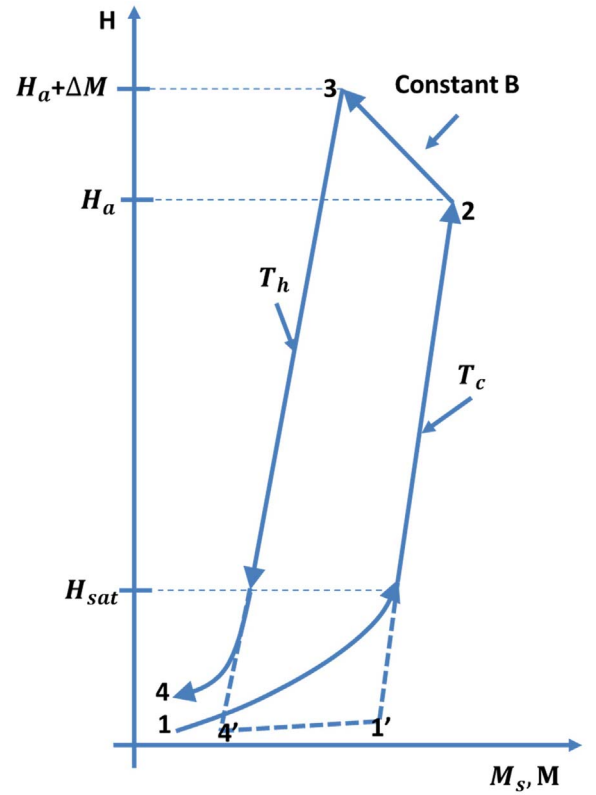


Fig. 7. The magnetic cycle of thermomagnetic generator. The figure is reconstructed from reference [18] for illustration.

tions, $M_s \approx M$ can be considered for the entire cycle. At the start of cycle 1'–2–3–4', the state of material is defined as 1'. The ferromagnetic material is in contact with heat sink, its temperature is T_c , applied voltage and magnetic field H is zero, and magnetization level is M_s . As voltage v_0 is applied by the voltage source, the magnetic field increases at constant rate changing the state of ferromagnetic material from 1' to 2. Heat is generated in material due to magneto-caloric effect, which is absorbed by cold reservoir isothermally.

At point 2, when $H = H_a$, voltage is set to zero. However, since resistance of superconducting coil is almost zero, current continues to flow. At this stage, the heat sink is disconnected and the heat source is connected to the ferromagnetic material, causing it to get heated from temperature T_c to temperature T_h at zero voltage. Increase in temperature in the ferromagnetic material results in decrease in its magnetization by ΔM . Voltage, magnetic induction, and magnetization are related to each other by Eqs. (10) and (12). From Eq. (10), for v to be zero, B must remain constant. Also, since B is constant, decrease in M must be compensated by increase in H . Therefore, when point 3 is reached, $H = H_a + \Delta M$. At this stage, voltage is reversed to $-v_0$, causing reversal in the current and in the direction of magnetic field. As the magnetic field decreases, the ferromagnetic material absorbs thermal energy from hot reservoir due to the magneto-caloric effect at constant temperature T_h . When the current and field reach almost zero at point 4', the voltage source is removed and the ferromagnetic material is allowed to cool to temperature T_c (point 1 or 1'). This ends the cycle. It can be noted that during step 1'–2, the voltage source supplies energy to magnetize the ferromagnetic material, and during steps 2–3 and 3–4, it absorbs energy as the ferromagnetic material gets demagnetized. During an entire cycle, there occurs a net gain in energy per unit volume, which is given by Eq. (17).

Solomon [18] used gadolinium as working material to evaluate the energy generated by thermomagnetic generator with cyclic magnetic field. The efficiency of thermomagnetic generator at various operating temperature cycles and magnetic fields are demonstrated using

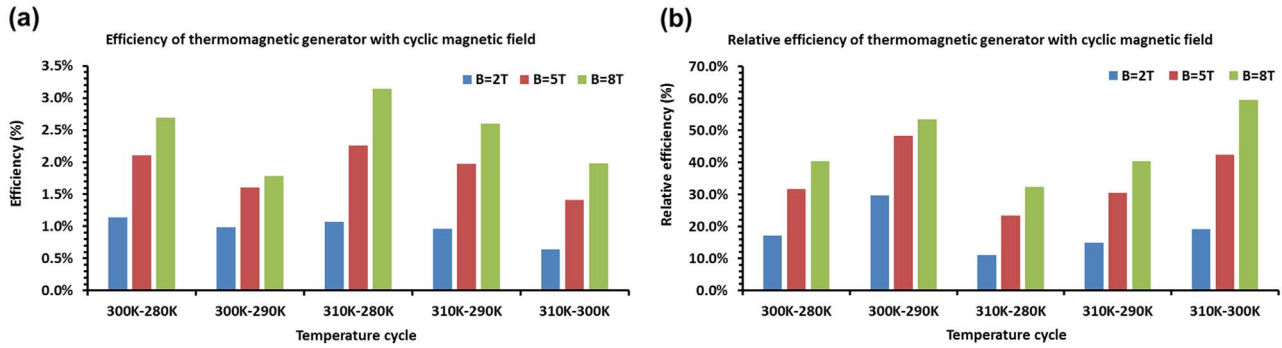


Fig. 8. (a). The absolute efficiency of thermomagnetic generator with cyclic magnetic field at different magnetic flux densities and thermal cycles. Data are taken from [18]. (b). The relative efficiency of thermomagnetic generator with cyclic magnetic field at different magnetic flux densities and thermal cycles. Data are taken from [18].

Figs. 8(a)–(b). Magnetic field B shown in Figs. 8(a)–(b) is constant B -line along path 2–3 of Fig. 7, and the relative efficiency shown in Fig. 8(b) is the efficiency of generator with respect to its Carnot efficiency.

Some important observations can be made from these figures. First, both efficiencies, absolute as well as relative, increase with increase in the magnetic field. Secondly, increasing ΔT has positive effect on the absolute efficiency. However, temperature needs to be cycled through Curie temperature and the maximum temperature T_h should be closer to Curie temperature (300K–280K cycle has higher efficiency than 310K–290K cycle and 300K–290K cycle has higher efficiency than 310K–300K cycle). Third, high relative efficiency may be possible with small ΔT and large T_h . However, it may not be the optimal case in regards to absolute efficiency. Lastly, thermomagnetic generator with cyclic magnetic field can obtain relative efficiency more than 55%, the theoretical limit for a normal thermomagnetic generator per Eq. (4).

4. Passive thermomagnetic devices

4.1. Working principle

Passive thermomagnetic devices are also called thermomagnetic motor or Curie motor or Curie point motor because they convert thermal energy into mechanical energy in form of rotary or linear motion. An electromechanical or electromagnetic device is needed to produce electricity. A thermomagnetic motor in its simplest form consists of a magnetic circuit with movable armature made-up of soft ferromagnetic material. Soft ferromagnetic materials generally have low Curie temperature. Curie temperature of a hard magnetic material based upon neodymium can be as high as 300 °C. It is therefore used to make permanent magnets as they remain magnetic in fairly large working range of temperature.

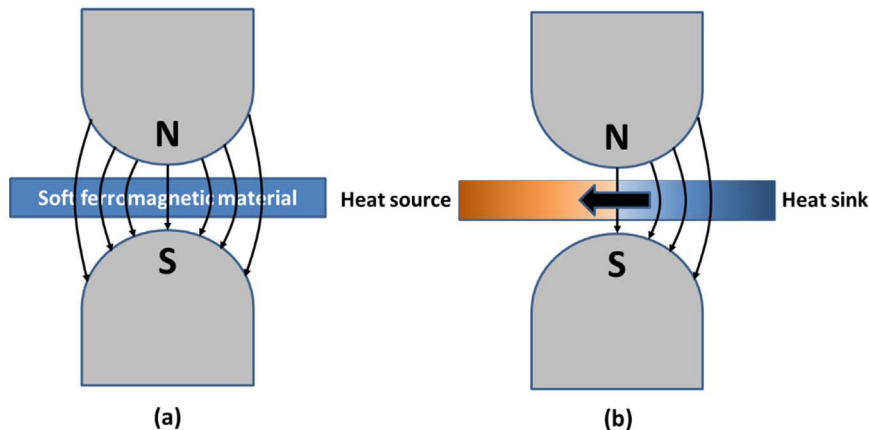


Fig. 9. Working principle of a thermomagnetic motor.

As shown in Fig. 9, when the entire armature is at a uniform temperature, the magnetic permeability is also uniform and the magnetic forces from the opposite directions are balanced. A portion of armature is now heated above the Curie temperature using a heat source, while the other portion in contact with the heat sink remains at low temperature, below the Curie point. This causes a permeability difference between hot and cold spots, producing a net unbalanced force on the armature. This results in linear or rotary motion of the armature. A restoring mechanism is needed to restore the initial condition for making hot-spot cold and cold-spot hot at a regular interval. This results in a cyclic motion.

4.2. Van Der Mass and Purvis's Curie point motor

In 1956, Van Der Mass and Purvis published a conceptual model of Curie point motor, as shown in Fig. 10 [19]. The device consists of a ferrite disk with diameter of 1.5" and thickness of 0.25". The disk is free to rotate about its axis between the poles of a permanent magnet. Region 1 of disk is surrounded by a D-shaped brass mantelpiece and region 2 is surrounded by a long narrow cooling mantle. Region 1 is heated above the Curie point of ferrite with a gas flame and at the same time region 2 is cooled using water. Region 1 loses its magnetization whereas region 2 remains magnetic, which leads to a moment on the disk. Curie point motor presented by Van Der Mass and Purvis was only a conceptual model and no quantitative tests were conducted. There was no information provided with regards to power output or efficiency of device.

4.3. Murakami and Nemoto's rotary thermomagnetic motor

Not much progress was made on thermomagnetic motor for a long time after Van Der Mass and Purvis proposed Curie point motor. After

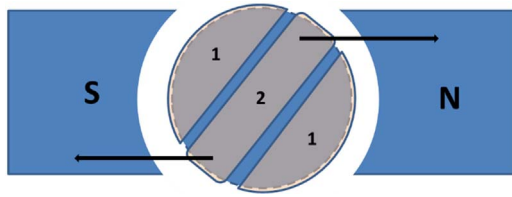


Fig. 10. Curie point motor presented by Van Der Mass and Purvis.

about 16 years, in 1972, Murakami and Nemoto published a study on performance of an experimental prototype of a rotary thermomagnetic motor [20]. They used a 500 mm diameter acrylic resin plate as the rotor of thermomagnetic motor. 65 pieces of 'temperature sensitive' magnetic material of dimension $2 \times 4.5 \times 20 \text{ mm}^3$ were arranged circumferentially at an equal interval on the outer surface of rotor. The Curie temperature of magnetic material was 50°C . Apart from this, no other information related to magnetic material was provided in the paper. A brass tank filled with silicon oil was used as the heat source at constant pre-set temperature. Ambient air was allowed to cool the heated magnetic piece, while ambient atmosphere acted as heat sink. Magnetic poles needed to generate working magnetic field were obtained using a C-shaped electromagnet with a wedge-shaped air-gap. The shape and key dimensions of electromagnet are shown in Fig. 11(a). Fig. 11(b) depicts the experimental set-up of device [20]. The performance of device given by mechanical power output P_o , thermal power input P_i , and efficiency η are shown in Fig. 11(c). It can be noted that the maximum thermal-to-mechanical energy conversion efficiency of the device is about 0.02%.

4.4. Takahashi's thermomagnetic engine

Takahashi et al. [21,22] presented triple magnetic circuit designs (triple-pole type) for rotary cylindrical and disk-type thermomagnetic engines, schematically depicted in Fig. 12. They used Nd-B-Fe for permanent magnets and temperature sensitive magnetic alloys, such as $\text{Fe}_{54}\text{Ni}_{36}\text{Cr}_{10}$ and $\text{Fe}_{68.5}\text{Ni}_{31.5}$, for rotor. Heating and cooling systems consisted of hydraulic nozzles that showered water at constant temperature of 95°C and 11°C , respectively. The studies claimed that optimized rotor consisting of 10 discs of 400 mm outer diameter, 40 mm width, and 0.5 mm thickness with a clearance of 1 mm is capable of producing mechanical power up to 14.8 W with a rotation speed of 0.76 revs per sec. Compared with the results from previous studies on similar devices, it was found that employing water as heating/cooling medium instead of air results in better heat transfer into the rotor and thus higher power output [21–23]. These studies further reveal that disk type thermomagnetic engine has lower eddy losses in comparison to a solid cylindrical thermomagnetic engine of the similar size; thus, former has higher power output.

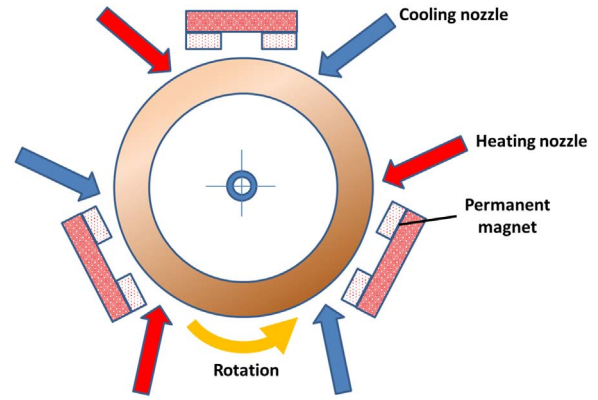


Fig. 12. Schematic diagram of Takahashi's thermomagnetic engine.

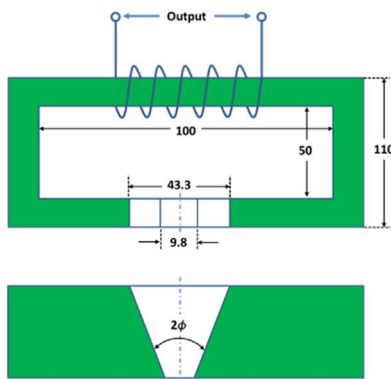
4.5. Palmy's floating thermomagnetic wheel

In 2006, Palmy published studies [24,25] on a passive thermomagnetic device called thermomagnetic wheel. The thermomagnetic wheel presented in his study is a floating disk-shaped magnet, which freely oscillates or rotates by the action of heat with no mechanical support. As shown in Fig. 13, the device consists of a small thin cylindrical NdFeB permanent magnet, 8 mm in diameter, 3 mm in thickness, and 1.2 g in weight, levitated between two poles of relatively larger size NdFeB permanent magnets. A diamagnetic material, Bismuth, is used to create a three-dimensional potential well, where stable levitation in free space is possible. The small magnet is placed by carefully adjusting the lifting magnets and diamagnetic bismuth plates so as to create a free-floating position. When the floating magnet is heated locally at the upper surface, it first oscillates with increasing amplitude. If the heating continues, it leads to permanent rotation. It is estimated that the rotational energy generated by the device is around $1\mu\text{J}$ with thermomechanical efficiency of around 0.01%.

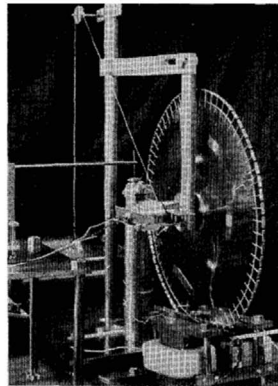
The thermal-to-mechanical conversion efficiency of thermomagnetic motor reported in literature has an efficiency less than 1%. If these devices are coupled to an electromechanical generator, the net efficiency would further decrease. No known attempt has been made to improve the performance of thermomagnetic motor using regenerative heating or any other methods. It should be noted here that thermomagnetic motor can be effectively used as thermomechanical actuator.

4.6. Thermomechanical actuator

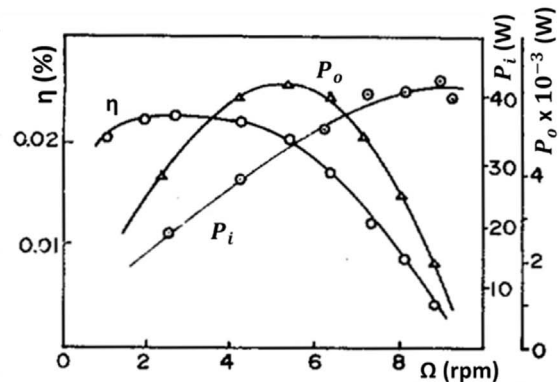
In 2007, Ujihara et al. [26] presented a novel thermomechanical actuator whose performance in terms of power density was found to be



(a)



(b)



(c)

Fig. 11. Murakami and Nemoto's rotary thermomagnetic motor. The figures are reconstructed from reference [20].

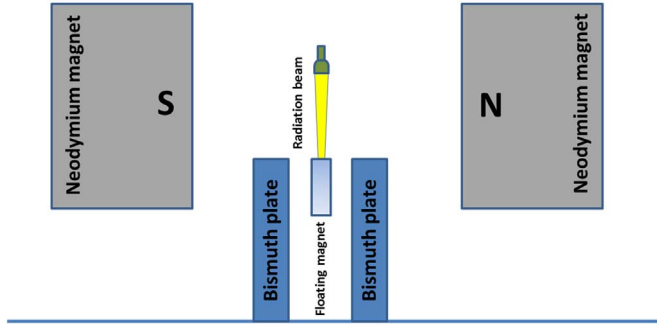


Fig. 13. Palmy's floating thermomagnetic wheel. The figure is reconstructed from reference [24,25].

close or better than the optimized thermoelectric converters. The conceptual model of Ujihara's device and its working mechanism are shown in Fig. 14. The working element of device is a soft (gadolinium) magnet, size $6\text{mm} \times 6\text{mm} \times 127\mu\text{m}$, suspended on a leaf spring near a relatively large permanent neodymium magnet. Initially when gadolinium magnet is below its Curie temperature, it is magnetic and is attracted by the permanent magnet. Soon however due to heat source, the temperature of gadolinium magnet rises above its Curie temperature, making it paramagnetic. It is then pulled away by the leaf spring and gadolinium magnet comes in contact with heat sink. Eventually, its temperature goes below the Curie temperature and it regains its magnetism. When the magnetic force is larger than the spring force, the permanent magnet pulls gadolinium magnet towards the heat source and the cycle continues.

Analytical and numerical modeling of this device has been presented by Bulgrin et al. [27] and Keyur and Priya [28]. A complete cycle of thermomagnetic actuator consists of three stages: First stage corresponds to the state when gadolinium is in contact with heat sink; second stage corresponds to state when gadolinium is in motion between heat sink and heat source under the combined influence of spring and magnetic forces; and in third stage gadolinium magnet is in contact with heat source. Therefore, the complete analysis of this device requires coupling three different models: (i) heat transfer model, (ii) magnetic model, and (iii) vibration model. In addition, if the device is being used to produce electricity, then a suitable electromechanical model is also required.

Theoretically, gadolinium experiences three forces: gravitational force (mg), spring force (F_s), and magnetic force (F_m). Since the mass of magnet is small, gravitational force is negligible in comparison to spring and magnetic forces. The equation of motion of gadolinium magnet can be given as:

$$F_s + F_m = -m \frac{d^2z}{dt^2} \quad (18)$$

The spring force F_s is calculated as:

$$F_s = K(l - z) \quad (19)$$

where K is spring constant, m is mass of gadolinium magnet, and l is maximum extension in the spring. Calculation of magnetic force F_m on a magnet in an external field B_{ext} is given as [28,29]

$$F_m = \int_V \nabla (M B_{ext}) dV \quad (20)$$

This can also be written as [29]:

$$F_m = - \int_V (\nabla \cdot M) B_{ext} dV + \int_s (M \cdot \hat{n}) B_{ext} dS \quad (21)$$

where \hat{n} is the unit surface-area vector.

The permanent neodymium magnet used for this device is magnetized along its thickness c (along z -axis as shown in Fig. 13) and has face area $2a \times 2b$. The magnetic flux density at distance z from the magnet surface, is given by [28,29]:

$$B(z) = \frac{B_r}{\pi} \left[\tan^{-1} \left(\frac{(z+c)\sqrt{a^2+b^2+(z+c)^2}}{ab} \right) - \tan^{-1} \left(\frac{y\sqrt{a^2+b^2+z^2}}{ab} \right) \right] \hat{z} \quad (22)$$

Also, the size of permanent magnet is considered relatively larger than the size of the gadolinium, so that the end effect can be ignored and magnetic flux density can be assumed to be constant in the x - y plane. The magnetization is a function of both external magnetic field as well as its temperature as is given as:

$$M = M_0 B_J \left(\frac{\mu_s (H + \gamma M)}{k_B T_a} \right) \hat{z} \quad (23)$$

where B_J denotes Brillouin function with the spin parameter J , which is equal to $7/2$ for the gadolinium material, M_0 is spontaneous- or self-magnetization at 0 K and k_B is the Boltzmann constant. Lastly, μ_s is the saturation magnetic moment per atom of the magnetic material. In case the external magnetic field is weak, magnetization can be considered a sole function of its temperature.

Next step is to obtain the temperature distribution in the gadolinium. Assuming uniform temperature in x - y plane, the temperature distribution along z -axis can be modeled using the equation:

$$\frac{\partial T}{\partial t} = \frac{\rho c_p}{k} \frac{\partial^2 T}{\partial z^2} \quad (24)$$

with boundary conditions

$$k \frac{\partial T}{\partial z} = -h_c (T - T_h) \text{ at } z = 0, \quad k \frac{\partial T}{\partial z} = h_c (T - T_c) \text{ at } z = z_0 \quad (25)$$

where ρ is density, c_p is specific heat, and k of thermal conductivity of gadolinium. Here z_0 is the gap between heat source and heat sink as shown in Fig. 14. Heat transfer through convection has been neglected.

All three models: thermal, magnetism, and vibration need to be solved simultaneously. This requires numerical techniques. Simulation results by Bulgrin [27] show that the optimized model of device is capable of producing mechanical power of 2.75 mW when hot surface temperature is 323 K and the cooling surface temperature is 273 K . The thermomechanical efficiency of the device is found to be around 3.7% . Considering mechanical to electrical energy conversion efficiency of piezoelectric materials in the range of $10\text{--}78\%$, the electrical power output of device is estimated to be between 0.275 mW and 2.145 mW . This corresponds to thermomagnetic efficiency of $0.37\text{--}2.9\%$.

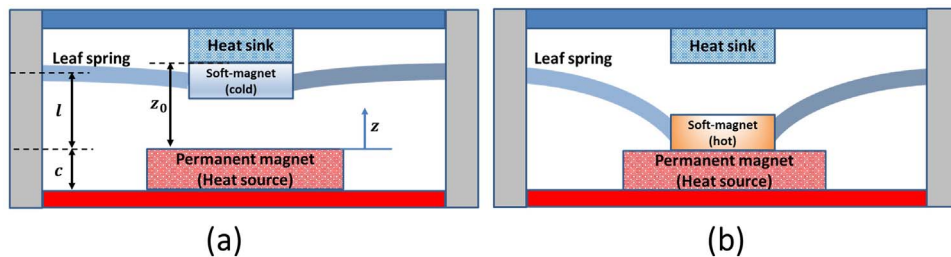


Fig. 14. Thermomechanical actuator by Ujihara et al. The figure is reconstructed from reference [26] for illustration.

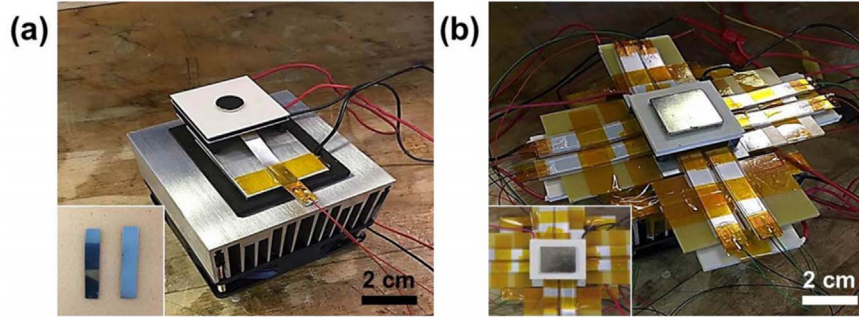


Fig. 15. Chun et al.'s thermo-magneto-electric generator (TMEG). (a) TMEG with a single bimorph cantilever and (b) TMEG with arrays of bimorph cantilevers.

4.7. Thermomagnetic device for active heat recovery system

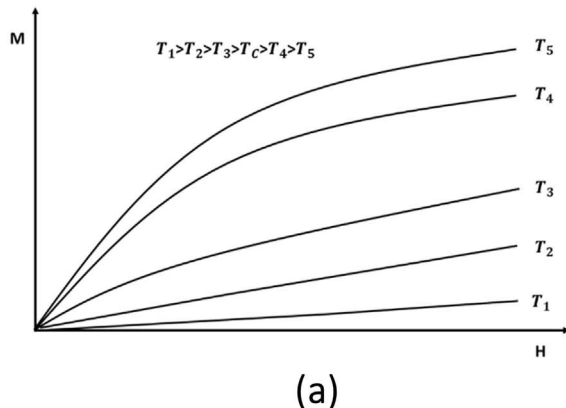
Chun et al. [15] have recently demonstrated that thermomagnetic devices can be used for generating power and also or enhancing the cooling rate of solar panels employed in unmanned aerial vehicles (UAVs). They also demonstrated the implementation of thermomagnetic devices for increasing the heat dissipation rate from data storage servers. Fig. 15 shows the structure of proposed thermo-magneto-electric generators (TMEGs) in this study [15]. The TMEG shown in Fig. 15(a) is composed of a single bimorph cantilever, whereas the TMEG shown in Fig. 15(b) consists of arrays of bimorph cantilevers. The working principle of TMEG is similar to thermomagnetic actuator discussed in previous section, except TMEG consists of flexible polyvinylidene difluoride (PVDF) bimorph cantilever instead of leaf spring. The study shows that TMEG with eight bimorph cantilever produces 158 μW output power. In addition, TMEG with a single bimorph cantilever increases the cooling rate by 1 $^{\circ}\text{C}$ per minute against the normal dissipation.

5. Materials for thermomagnetic energy harvesters

The performance of thermomagnetic generators is strongly dependent on the thermomagnetic properties of ferromagnetic material undergoing the thermomagnetic cycle. Fig. 16(a) shows the typical isothermal magnetization curves of a ferromagnetic material at different temperatures. If the thermo-magnetic cycle occurs between temperature T_1 and T_5 and magnetic field H_0 and H_a , then the shaded area shown in Fig. 16(b) represents the maximum obtainable energy from a thermomagnetic cycle. Using Eq. (17), the maximum work potential of a thermomagnetic generator can be given as:

$$w_{max} = E_{out} = \mu_0 \oint H dM \quad (26)$$

Eq. (1) provides the theoretical limit on the efficiency of a thermomagnetic generator as:



$$\eta_{max} = \frac{w_{max}}{q_{in}} = \frac{\mu_0 \oint H dM}{q_{in}} \quad (27)$$

Following the first law of thermodynamics, the heat input to a system is equal to the sum of increase in internal energy and the work done by system. For a ferromagnetic material, the change in internal energy is associated with two effects: (i) change in temperature and (ii) change in magnetic entropy. Therefore,

$$q_{in} = \rho \int_{T_c}^{T_h} C_p(T) dT + T \int dS_m \quad (28)$$

where C_p is the specific heat for material and S_m is the magnetic entropy.

When the applied magnetic field H is small, the first term $\rho \int_{T_c}^{T_h} C_p(T) dT$ is much larger than $T \int dS_m$, and therefore later can be ignored [30,31]. Efficiency (or absolute efficiency) of a thermomagnetic cycle can be defined as:

$$\eta(\text{or } \eta_{abs}) \cong \frac{\mu_0 \oint H dM}{\rho \int_{T_c}^{T_h} C_p(T) dT} \quad (29)$$

The relative efficiency with respect to Carnot efficiency of a thermomagnetic cycle can be given as:

$$\eta_{rel} = \frac{\eta_{abs}}{\eta_{carnot}} = \frac{\eta_{abs}}{1 - \frac{T_c}{T_h}} \quad (30)$$

The absolute efficiency and relative efficiency are function of several magneto-thermal parameters: the range of applied magnetic field (H_0 , H_a), the magnetization curve at cold temperature $T = T_c$, specific heat that is function of temperature, Curie temperature T_c , and cold and hot state temperatures T_c and T_h . The magnetization at temperature $T_h > T_c$ is small, therefore it can be ignored.

Effect of magnetic field on efficiency was discussed in previous sections. Normally efficiency of thermomagnetic cycle increases with

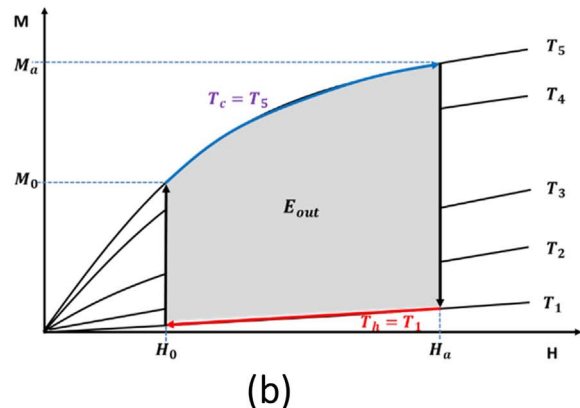


Fig. 16. (a) Typical isothermal magnetization curves of a ferromagnetic material, and (b) the maximum obtainable energy from a thermomagnetic cycle.

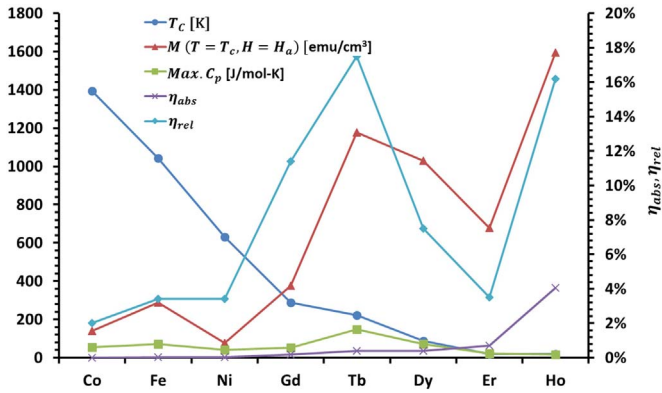


Fig. 17. Absolute efficiency and relative efficiency calculated for various polycrystalline ferromagnetic elements: Co, Fe, Ni, Gd, Tb, Dy, Er, and Ho) in a thermomagnetic cycle operating at magnetic field $H_a = 3000\text{Oe}$ and at temperature cycle between T_C and $T_C + 5\text{K}$ or $T_C - 5\text{K}$. All units are in CGS. Data are taken from [30].

increase in applied magnetic field, and therefore employing stronger magnet improves the performance of thermomagnetic generator. Fig. 17 shows the effect of other parameters on absolute and relative efficiency calculated for various polycrystalline ferromagnetic elements (Co, Fe, Ni, Gd, Tb, Dy, Er, and Ho) in a thermomagnetic cycle operating at magnetic field $H_a = 3000\text{Oe}$ and at temperature cycle between T_C and $T_C + 5\text{K}$ or $T_C - 5\text{K}$. It can be noted that the absolute efficiency has an inverse relationship with Curie temperature of magnetic materials; absolute efficiency increases with decrease in Curie temperature. The relative efficiency seems to follow the similar trend as magnetization of material at $T = T_C$ and $H = H_a$. It should be noted that Fe, Co, Ni, and Gd transform from a ferromagnetic to paramagnetic phase at Curie point, whereas Tb, Dy, Ho, and Er undergo ferromagnetic to antiferromagnetic phase transition. Ferromagnetic to antiferromagnetic phase transition is an order-to-order phase transformation, whereas ferromagnetic to paramagnetic phase transition in order-to-disorder phase transformation. The order-to-order phase transformation normally is associated with better thermomagnetic efficiency than the order-to-disorder phase transformation. This happens because relatively larger amount of magnetic energy is lost to entropy during the transition from an ordered to a disordered state as compared to ordered to ordered state transition [30].

In Fig. 18, the performance of single crystal and polycrystal forms have been compared for Gd, Tb, Dy, and Ho. In all cases, single crystal materials have higher absolute and relative efficiencies than their polycrystalline forms for the same thermomagnetic cycle. This is due to the fact that single crystal materials have higher susceptibility and thus larger magnetization than the polycrystals under the same

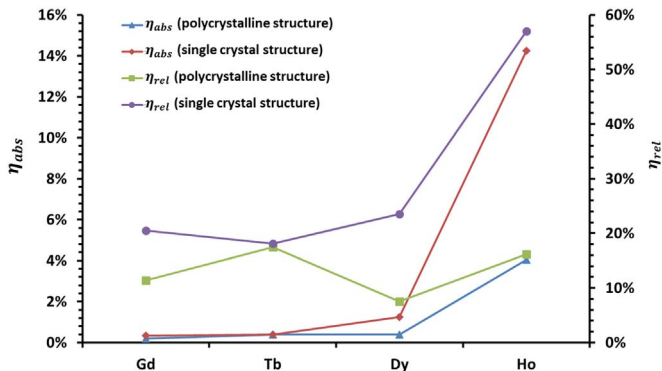


Fig. 18. Comparison between performance of single crystalline and polycrystalline materials for the same element under the same thermomagnetic cycle ($\Delta T = 5\text{K}$ and $H_a = 3000\text{Oe}$). Data taken from reference [30].

external field. Single crystal materials exhibit magnetic anisotropy, and thus under applied magnetic field, the spins are aligned more easily along an easy direction in comparison to the polycrystals [30]. It can be noticed that single crystals and order-to-order transitions result in relatively higher efficiency than polycrystals and order-to-disorder transitions. Hsu et al. have suggested that by reducing randomness, either structural or magnetic disorder in ferromagnetic materials, the thermomagnetic energy harvesting efficiency can be improved.

Out of various elements discussed above, Gd is the most popular material because its thermomagnetic efficiency has been found to be much better than the conventional ferromagnetic materials. Gd is normally paramagnetic at room temperature and thus it requires a heat sink (or a refrigerator) to operate in a thermomagnetic cycle. Generally, heat sources are more conveniently available (for example, in the form of waste heat). A potential solution to this problem could be the multiferroic Heusler alloy, $\text{Ni}_{45}\text{Co}_5\text{Mn}_{40}\text{Sn}_{10}$. The use of this material for the conversion of heat into electricity was demonstrated by Srivastava et al. [32]. The Heusler alloy undergoes first order transition from a strongly ferromagnetic austenite phase to a weakly ferromagnetic martensite phase at critical temperature of 408 K [33,34], unlike Gd, that shows second order phase transition from ferromagnetic to paramagnetic state. The thermal energy requirement at critical temperature for first order phase transformation is dominated by latent heat, whereas the second order phase transition is mainly governed by sensible heat. Therefore, Heusler alloy needs larger heat input per thermomagnetic cycle than gadolinium.

Post et al. [31] studied the performance of Heusler alloy between the temperature range of 403 K and 408 K under external field ranging from 0 Oe to 3000 Oe. Table 3 compares the absolute and relative efficiency of Heusler alloy and other materials discussed above. It can be seen that Heusler alloy exhibits absolute efficiency of 0.2% and relative efficiency of 15.9%, which is between the performance of polycrystalline gadolinium ($\eta_{abs} = 0.19\%$, $\eta_{rel} = 11.4\%$) and single crystal gadolinium ($\eta_{abs} = 0.34\%$, $\eta_{rel} = 20.5\%$) under similar operating conditions. Post et al. [31] continued their study to evaluate performance of Heusler alloy for passive type of thermomagnetic device. They used thermomagnetic actuator of similar size as that presented by Ujihara et al. [26] discussed in previous section. Heusler alloy was found to provide better power density and efficiency in comparison to gadolinium.

Another study by Solomon [35] recommends $\text{Y}_2(\text{Fe}_x\text{Co}_{1-x})_{17}$ as the working ferromagnetic material for thermomagnetic generator. Some studies [18,35] have shown that Curie temperature of $\text{Y}_2(\text{Fe}_x\text{Co}_{1-x})_{17}$ can be changed from 324 K to 1250 K by varying the concentration of iron and cobalt (value of x) from 1 to 0 in the alloy. This gives us the flexibility to vary the Curie temperature according to thermal condition

Table 3
Thermomagnetic cycle efficiencies of ferromagnetic materials [30,31].

Elements	Curie temperature (T_C) [K]	Magnetic phase transition	T_h [K]/ T_c [K] ($\Delta T = 5\text{K}$)	η_{Carnot} [%]	η_{rel} [%]
Co	1394	Ferro-Para	1394/1389	0.36	2.0
Fe	1044	Ferro-Para	1044/1039	0.49	3.4
Ni	630	Ferro-Para	630/625	0.79	3.4
Heusler alloy	408	Ferro-Ferro	408/403	0.2	15.9
Gd (poly)	288	Ferro-Para	288/283	1.71	11.4
Gd (single)	294	Ferro-Para	294/289	1.67	20.5
Tb (poly)	221	Ferro-Anti	221/216	2.21	17.5
Tb (single)	221	Ferro-Anti	221/216	2.21	18.1
Dy (poly)	89	Ferro-Anti	89/84	5.32	7.5
Dy (single)	89	Ferro-Anti	89/84	5.32	23.5
Ho (poly)	20	Ferro-Anti	20/15	25	16.2
Ho (single)	20	Ferro-Anti	20/15	25	57
Er (poly)	20	Ferro-Anti	20/15	20	3.5
Er (single)	20	Ferro-Anti	20/15	20	65.1

of the working environment. In addition to gadolinium and Heusler alloy, there are several other thermomagnetic materials, which have been found to exhibit thermomagnetic response. Some of these materials are Gd-based alloys such as $\text{Gd}_5\text{Si}_2\text{Ge}_2$ [36], GdFe_6Al_6 [37] and other binary and ternary compounds [38–40], MnAs and its related compounds [41–43], and lanthanide transition-metal-based compounds [44–49]. Most of these materials undergo a first-order phase transition at a critical temperature and exhibit giant magnetic entropy change. However, the performance of these materials for applications in thermomagnetic devices has not been examined and it is a potential area of research.

6. Conclusion

In conclusion, thermomagnetic energy harvesters hold a great potential, especially for the cases where power generation from low-grade or waste heat is required. The gadolinium based thermomagnetic generators (active devices) have been found to exhibit efficiency as high as 20.5% of the Carnot efficiency for an operating condition near room temperature with a temperature gradient of only 5 K and magnetic field up to 3000 Oe, which is easily achievable using neodymium based permanent magnets. Prior studies have shown that the performance of these devices can be further increased up to 75% of Carnot efficiency by applying stronger magnetic field. Theoretical models can be used to optimize the thermomagnetic generators based on the operating conditions including magnetic field, operating temperature, and thermal gradient.

Passive thermomagnetic devices such as thermomagnetic motors or actuators have poorer performance as compared to the active device. However, passive devices can be used very effectively as an actuator or where linear or rotational motion is needed continuously. In addition, passive thermomagnetic devices can be used to enhance the cooling or heat-dissipation rate of a hot object such as solar panels or data servers.

Selection of suitable thermomagnetic material is key requirement. Ferromagnetic materials with low Curie temperature generally have better efficiency. Conventional ferromagnetic materials such as iron and cobalt have Curie temperature above 1000 K and this was the reason behind the failure of prior thermomagnetic generators. Gadolinium is most suitable for the purpose since its Curie temperature is close to room temperature; however, it requires a heat sink or a refrigerator since the operating temperature needs to be between Curie temperature and further lower temperature. Heusler alloys have been recently found as promising alternative material.

Acknowledgments

R.K. acknowledges the financial support from ICTAS Doctoral Scholars Program and AMRDEC. S.P. is thankful for the support from office of basic energy science, department of energy through grant number DE-FG02-06ER46290.

References

- [1] Kong LB, Li T, Hng HH, Boey F, Zhang T, Li S. Waste energy harvesting. Springer; 2014.
- [2] Rowe DM. Thermoelectrics, an environmentally-friendly source of electrical power. *Renew Energy* 1999;16:1251–6.
- [3] Rowe D, Min G. Evaluation of thermoelectric modules for power generation. *J Power Sources* 1998;73:193–8.
- [4] Elsheikh MH, Shnawah DA, Sabri MFM, Said SBM, Hassan MH, Bashir MBA, et al. A review on thermoelectric renewable energy: principle parameters that affect their performance. *Renew Sustain Energy Rev* 2014;30:337–55.
- [5] Zhan G-D, Kuntz JD, Mukherjee AK, Zhu P, Koumoto K. Thermoelectric properties of carbon nanotube/ceramic nanocomposites. *Scr Mater* 2006;54:77–82.
- [6] Tesla N. in: Patent#396121 U, editor; 1889.
- [7] Edison TA. Pyromagnetic motor. in: Patent#380100 U, editor; 1888.

- [8] Tesla N. Pyromagneto-electric generator. in: Patent#428057 U, editor; 1890.
- [9] Edison TA. Pyromagnetic generator. in: Patent#476983 U, editor; 1892.
- [10] Elliott J. Thermomagnetic generator. *J Appl Phys* 1959;30:1774–7.
- [11] Roderback GW, USAECTI Center. North American aviation. *At Int D Thermomag Gener* 1953.
- [12] Stauss H. Efficiency of thermomagnetic generator. *J Appl Phys* 1959;30:1622–3.
- [13] Kirol LD, Mills JI. Numerical analysis of thermomagnetic generators. *J Appl Phys* 1984;56:824–8.
- [14] Paradiso JA, Starner T. Energy scavenging for mobile and wireless electronics. *IEEE Pervasive Comput* 2005;4:18–27.
- [15] Chun J, Song H-C, Kang M-G, Kang HB, Kishore RA, Priya S. Thermo-magneto-electric generator arrays for active heat recovery system. *Sci Rep* 2017;7:41383.
- [16] Bozorth RM. Ferromagnetism. In: Bozorth Richard M, editor. , 1. Wiley-VCH; 1993. p. 992.
- [17] Nigh HE, Legvold S, Spedding F. Magnetization and electrical resistivity of gadolinium single crystals. *Phys Rev* 1963;132:1092.
- [18] Solomon D. Improving the performance of a thermomagnetic generator by cycling the magnetic field. *J Appl Phys* 1988;63:915–21.
- [19] GJvd Maas, Purvis WJ. “Curie point” motor. *Am J Phys* 1956;24:176–7.
- [20] Murakami K, Nemoto M. Some experiments and considerations on the behavior of thermomagnetic motors. *IEEE Trans Magn* 1972;8:387–9.
- [21] Takahashi Y, Matsuzawa T, Nishikawa M. Fundamental performance of the disc-type thermomagnetic engine. *Electr Eng Jpn* 2004;148:26–33.
- [22] Takahashi Y, Yamamoto K, Nishikawa M. Fundamental performance of triple magnetic circuit type cylindrical thermomagnetic engine. *Electr Eng Jpn* 2006;154:68–74.
- [23] Takahashi Y, Irie T, Nishikawa M. Experiment on cylindrical thermomagnetic engine for exhaust heat recovery. *IEEJ Trans Power Energy* 2003;123:389–94.
- [24] Palmy C. A new thermo-magnetic wheel. *Eur J Phys* 2006;27:1289.
- [25] Palmy C. A thermo-magnetic wheel. *Europhys News* 2007;38:32–4.
- [26] Ujihara M, Carman G, Lee D. Thermal energy harvesting device using ferromagnetic materials. *Appl Phys Lett* 2007;91:093508.
- [27] Bulgrin KE, Ju YS, Carman GP, Lavine AS. A coupled thermal and mechanical model of a thermal energy harvesting device. *ASME 2009 International Mechanical Engineering Congress and Exposition. American Society of Mechanical Engineers*; 2009. p. 327–35.
- [28] Joshi KB, Priya S. Multi-physics model of a thermo-magnetic energy harvester. *Smart Mater Struct* 2013;22:055005.
- [29] Furlani EP. Permanent magnet and electromechanical devices: materials, analysis, and applications. Academic press; 2001.
- [30] Hsu C-J, Sandoval SM, Wetzlar KP, Carman GP. Thermomagnetic conversion efficiencies for ferromagnetic materials. *J Appl Phys* 2011;110:123923.
- [31] Post A, Knight C, Kisi E. Thermomagnetic energy harvesting with first order phase change materials. *J Appl Phys* 2013;114:033915.
- [32] Srivastava V, Song Y, Bhatti K, James R. The direct conversion of heat to electricity using multiferroic alloys. *Adv Energy Mater* 2011;1:97–104.
- [33] Song Y. Performance analysis of energy conversion via caloric effects in first-order ferroic phase transformations. *Phys Chem Chem Phys* 2014;16:12750–63.
- [34] Song Y, Bhatti KP, Srivastava V, Leighton C, James RD. Thermodynamics of energy conversion via first order phase transformation in low hysteresis magnetic materials. *Energy Environ Sci* 2013;6:1315–27.
- [35] Solomon D. Design of a thermomagnetic generator. *Energy Convers Manag* 1991;31:157–73.
- [36] Pecharsky VK, Gschneidner KA, Jr. Giant magnetocaloric effect in $\text{Gd}_5(\text{Si}_2\text{Ge}_2)$. *Phys Rev Lett* 1997;78:4494.
- [37] Klimczak M, Talik E. Magnetocaloric effect of GdTX ($T = \text{Mn, Fe, Ni, Pd, X} = \text{Al, In}$) and GdFe_6Al_6 ternary compounds [Conference Series: IOP Publishing]. *J Phys* 2010;092009.
- [38] Law J, Ramanujan R, Franco V. Tunable Curie temperatures in Gd alloyed Fe–B–Cr magnetocaloric materials. *J Alloy Compd* 2010;508:14–9.
- [39] Canepa F, Napolitano M, Cirafici S. Magnetocaloric effect in the intermetallic compound Gd_7Pd_3 . *Intermetallics* 2002;10:731–4.
- [40] Spichkin Y, Pecharsky V, Gschneidner K, Jr. Preparation, crystal structure, magnetic and magnetothermal properties of $(\text{Gd} \times \text{Gd} \times \text{R} 5 - \text{x} 5 - \text{x}) \text{Si} 4$, where $\text{R} = \text{Pr}$ and Tb , alloys. *J Appl Phys* 2001;89:1738–45.
- [41] Von Ranke P, De Oliveira N, Gama S. Theoretical investigations on giant magnetocaloric effect in $\text{MnAs} 1 - \text{x} \text{Sb} \text{x}$. *Phys Lett A* 2004;320:302–6.
- [42] Wada H, Morikawa T, Taniguchi K, Shibata T, Yamada Y, Akishige Y. Giant magnetocaloric effect of $\text{MnAs} 1 - \text{x} \text{Sb} \text{x}$ in the vicinity of first-order magnetic transition. *Phys B: Condens Matter* 2003;328:114–6.
- [43] Wada H, Taniguchi K, Tanabe Y. Extremely large magnetic entropy change of $\text{MnAs} 1 - \text{xSb} \text{x}$ near room temperature. *Mater Trans* 2002;43:73–7.
- [44] Das S, Dey T. Magnetic entropy change in polycrystalline $\text{La} 1 - \text{x} \text{K} \text{x} \text{MnO} 3$ perovskites. *J Alloy Compd* 2007;440:30–5.
- [45] Zhong W, Chen W, Au C, Du Y. Dependence of the magnetocaloric effect on oxygen stoichiometry in polycrystalline $\text{La} 2/3 \text{Ba} 1/3 \text{MnO} 3 - \delta$. *J Magn Magn Mater* 2003;261:238–43.
- [46] Hanh D, Islam M, Khan F, Minh D, Chau N. Large magnetocaloric effect around room temperature in $\text{La} 0.7 \text{Ca} 0.3 - \text{xPb} \text{xMnO} 3$ perovskites. *J Magn Magn Mater* 2007;310:2826–8.
- [47] Phan M-H, Tian S-B, Yu S-C, Ulyanov A. Magnetic and magnetocaloric properties of $\text{La} 0.7 \text{Ca} 0.3 - \text{xBa} \text{x} \text{MnO} 3$ compounds. *J Magn Magn Mater* 2003;256:306–10.
- [48] Sun W, Li J, Ao W, Tang J, Gong X. Hydrothermal synthesis and magnetocaloric effect of $\text{La} 0.7 \text{Ca} 0.2 \text{Sr} 0.1 \text{MnO} 3$. *Powder Technol* 2006;166:77–80.
- [49] Li J, Sun W, Ao W, Tang J. Hydrothermal synthesis and magnetocaloric effect of $\text{La} 0.5 \text{Ca} 0.3 \text{Sr} 0.2 \text{MnO} 3$. *J Magn Magn Mater* 2006;302:463–6.